The Results of Experiment on the Liquefaction of Saturated Sands with a Shaking Box: Comparison with Other Methods

Sukeo O-HARA*

(Received November 28, 1972)

Abstract

For the experimental study of liquefaction of saturated sands by shaking, there are generally two methods. One is by dynamic triaxial and dynamic simple shear tests, and the other is by means of a sand box on the shaking table. However, each has its merits and demerits. The major drawback with the latter method is that the stress conditions in the sand box cannot be regulated strictly. To cope with this problem, the author contrived a means of applying the consolidating pressure by use of compressed air, in order to reduce the disadvantage to some extent. In this experiment, it was confirmed that, for a given apparent density of the sand, the occurrence of its liquefaction is also determined by the ratio of shearing stress in the sand and initial effective pressure.

Then, in order to evaluate the experimental results by a shaking sand box; both dynamic triaxial and simple shear tests were also made for the same kinds of sands, thereby comparing between the three respective techniques.

The differences in the angle of internal friction at the time of a liquefaction were further examined for these methods.

As a result, it was found that the shearing stress required for liquefaction is largest with the shaking box test, followed by dynamic triaxial test and dynamic simple shear test in decreasing order.

Introduction

To study experimentally the liquefaction of saturated sands due to shaking, two methods are generally used. One is by dynamic triaxial compression and dynamic simple shear tests in which shearing force is repeatedly applied to the test sample. And the other is by means of a sand box on the shaking table: the saturated sand in the box is thus subjected to shaking.

The former two techniques were developed by Seed et al[1]. These have the advantage that during an experiment the stress conditions in the test sample can be controlled definitely. The dynamic correlations in mechanism of the liquefaction can thus be clarified experimentally. There is however problem in the similarity to actual ground under the stressed condition. In this respect, the latter method by a sand box is advantageous, in obtaining the response to shaking for example, since the sand layer in the box can be taken so-to-speak as a miniature ground. The method, however, has also a number of draw-

* Department of Civil Engineering

backs. These include the effect of shape and size of the shaking sand box, the difficulty in regulating the confining pressure to the sand, and near inability of knowing directly the repeated shearing stress in the sand at the time of its shaking. The drawbacks to the shaking box method are rather numerous, compared to the former two techniques.

In the shaking sand box method, however, the liquefaction in sand layer can be observed directly and further the pore pressure distribution in the direction of depth is also measurable. With these advantages, it is therefore used presently.

In the author's experiment with a shaking sand box, a rubber membrane was placed on the surface of sand layer and compressed air was applied on to it. In this way, the effect of this effective normal pressure on the liquefaction was observed. These results have been reported in a previous paper[2].

Subsequently, in order to assess the results obtained by a shaking sand box, experiments by the other two techniques were made for the same sands, and the results were together comparatively studied. In the present paper, these findings followed with discussion are described.

Experiment with a shaking sand box, and the results

In the present report, description is mainly of the comparison in results of the other two techniques and the method by a sand box. Therefore, the experiment and results by the latter method, described fully in the previous report, will be given briefly below.

The sand box, of steel plate, placed on the shaking table, is 100 cm in length by 58 cm wide by 30 cm deep. Saturated sand is filled into it, and the surface is smoothed evenly. A rubber membrane, 1 mm in thickness, is placed on it, then the box is closed with a top lid, being tightened to the box at the periphery. Compressed air is introduced into the air-tight space between top lid and rubber membrane, to consolidate the sand layer (Fig. 1). In this case, the effective

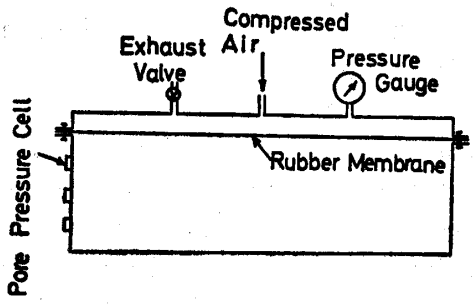

Fig. 1. Shaking sand box

normal pressure on to the sand layer is equal to the compressed air pressure. Under this condition, shaking is applied to the sand through a shaking table until occurrence of the liquefaction. Change in the pore pressure in the sand

layer is then also measured.

Application of the shaking acceleration is by either of the following two.

(1) The acceleration is incereased at a constant rate until the liquenfaction takes place.

(2) The shaking of a specific acceleration is applied until occurrence of the liquefaction.

With the procedure (1) above, the relation between the shaking acceleration necessary for the liquefaction and the effective pressure can be known. With the procedure (2), on the other hand, the shaking duration required for occurrence of the liquefaction in shaking at a given acceleration can be obtained.

In the previous experiment, the two kinds of sands described later in this report were used.

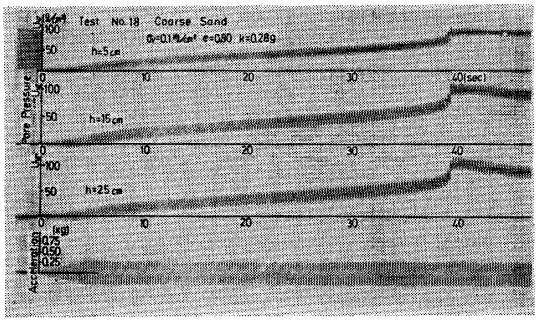

Fig. 2. Record of shaking table test

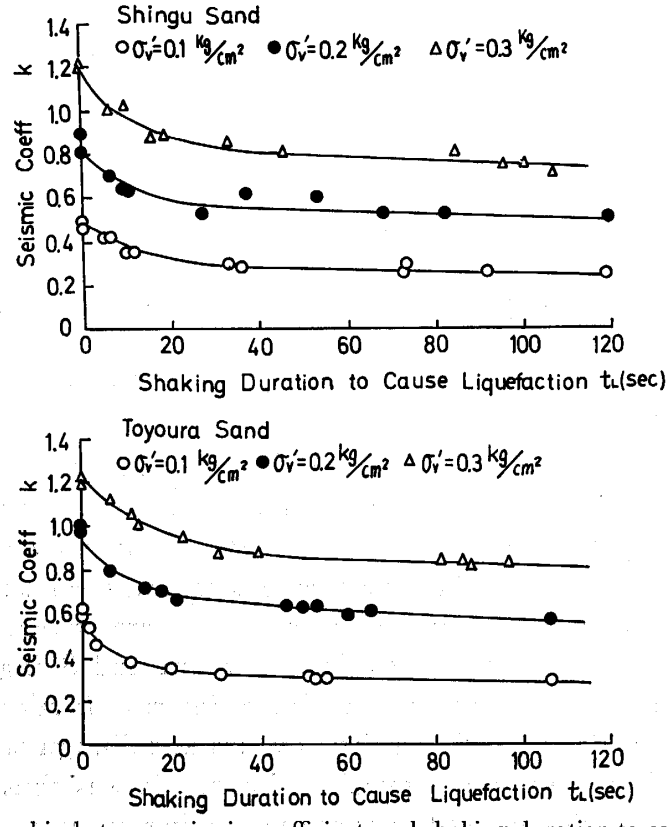

Fig. 3. Relationship between seismic coefficient and shaking duration to cause liquefaction

Figure 2 shows the results by the procedure (2), for example. In the figure, the four curves correspond to changes in the pore pressure at depth 5, 15 and 25 cm respectively and the shaking accelerations. It is seen that the pore pressures increase abruptly at about 60 sec after start of the shaking; liquefaction of the sand has evidently occurred at this point.

From the results, the relation between seismic coefficient and the shaking duration causing the liquefaction is plotted in Fig. 3 for the respective, initial effective normal pressures. The seismic coefficient for causing the liquefaction is seen to be in proportion to the initial effective pressure.

The normal effective pressure just before occurrence of the liquefaction is in linear relation with the seismic coefficient, as shown in Fig. 4.

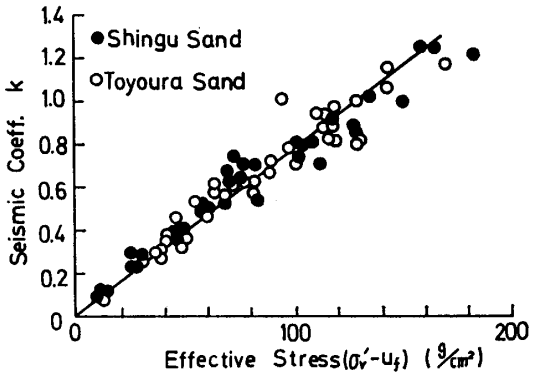

Fig. 4. Relationship between effective stress and seismic coefficient

Due to the linear relations such as above, the following can be formulated as the conditions for liquefaction.

$$\tau_d = (\sigma'_v - U_f) \tan\phi \qquad (1)$$

Here, τ_d : Shearing stress due to the shaking
σ'_v : Initial, effective normal pressure
U_f : Pore pressure just before occurrence of the liquefaction
ϕ : The angle of internal friction

The expression (1) is considered, for τ_d and seismic coefficient k in the shaking can be in linear relation.

If the degree of internal friction in eq. (1) can be known, from the relation in Fig. 4, the relation of k and τ_d for the sand layer in the shaking box is obtained. Then, replacing the quantity in the vertical axis of Fig. 3 by τ_d/σ'_v, the values for different σ'_v can be plotted. In the previous report, the results with $\phi=20°$, by referring to Bjellum's experimental results, were given. Subsequently, in the triaxial test for the same sands, ie. Toyoura and Shingu, of which the results will be described shortly, the sangles of internal friction were obtained as 34° (e=0.85) and 30° (e=0.82) for the Toyoura and Shingu sands respectively. The results with these values are given in Fig. 5. It was thus confirmed that occurrence of the liquefaction and further the shaking duration causing this can

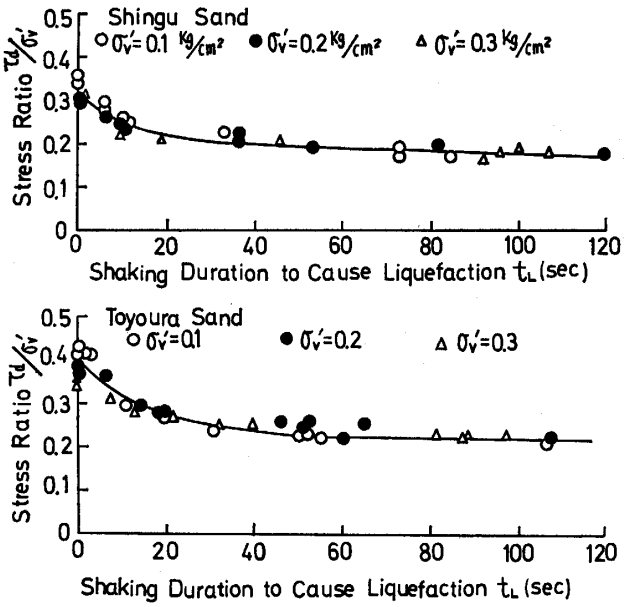

Fig. 5. Stress ratio τ_d/σ'_v required to cause liquefaction

both be simply determined by the stress ratio τ_d/σ'_v.

The above is a summary of the results in the previous report. It was shown that the influence by the effective pressure on the liquefaction of saturated sands can also be known by the experiment with a shaking sand box.

Sands

Due to the purpose of the present study, experiments were made for the same two kinds of sands as used in the previous experiment with a shaking sand box. Various factors and the grain size distributions for the two sands are shown in Table 1 and Fig. 6, respectively. Both the sands are relatively uniform in grain size; one (the Toyoura sand) is comparatively fine and the other (the Shingu sand) is coarse. The void ratios, as both the sands are filled into shaking boxes as saturated, are 0.85 and 0.82 (for the Toyoura and the Shingu sands) respectively, as described in the previous report. In the present experiment, therefore, an attempt was made to have the same values.

Table 1. Soil properties of Toyoura fine sand and Shingu coarse sand used in this tests

	Toyoura Sand	Shingu Sand
Specific Gravity G_s	2.63	2.64
50% Grain Size D_{50}	0.23 mm	0.82 mm
Uniformity Coeff. Cu	1.44	1.36
Max. Void Ratio e_{max}	1.06	0.58
Min. Void Ratio e_{min}	0.70	0.58

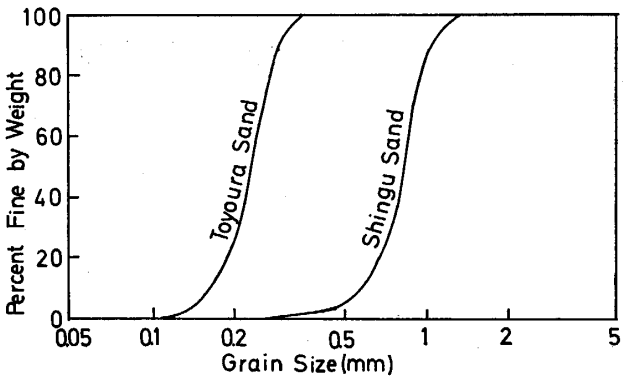

Fig. 6. Grain size distribution curves

The angles of internal friction shown in Table 1 were obtained by consolidated undrained triaxial test.

Experimental apparatuses

The apparatuses used in experiments are a dynamic triaxial apparatus and a dynamic simple shear apparatus.

Dynamic triaxial apparatus It is shown in Fig. 7. The test sample is 3.5 cm

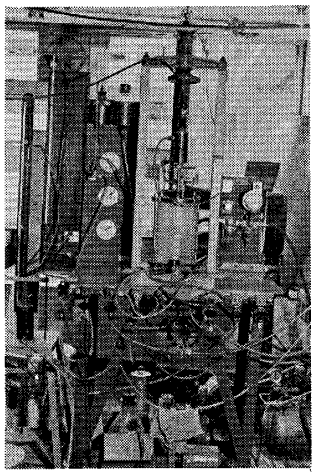

Fig. 7. Dynamic triaxial test apparatus

in diameter and about 8.0 cm high. The sample is consolidated at a specific confining pressure, and the sample as confined is then subjected to teported deviator stress of a given amplitude at a specific frequency.

For this purpose, the spindle to which the upper pressure plate is connected is joined to the piston rod a air-cylinder: compressed air is introduced in or removed from the upper and lower chambers alternately. The time intervals of this feeding and exhaust are controlled by means of a solenoid valve and the associated relay circuit. The air pressure introduced into the cylinder is regulated in advance by a reducing valve. The air cylinder used is a bello-phragm

cylinder; it is of such a special mechanism that the friction between piston and cylinder and between piston rod and bearing are nearly zero. Its effective sectional area is 17.7 cm^2.

Amplitude of the deviator stress is measured by a transducer of the wire strain gauge type which is attached to a rod supporting the air cylinder. Axial strain of the sample is then observed through displacement of the spindle measured by a differential transformer type diaplacement meter. For the measurement of pore pressure in the sample, the pressure water penetrating through a porous plate in the pedestal is led to a suitable point through a copper pipe: the measurement is made with a pressure cell of diaphragm 6 cm in diameter. This pressure cell is also of the wire strain gauge type.

Feeding of compressed air to the cylinder and its exhaust are controlled by the solenoid valve, and so the deviator stress is applied in square waves; the frequency is 0.5 c/s.

Dynamic simple shear apparatus The apparatus was prepared in the author's laboratory; its shearing box is of the same type as Kjellman's.

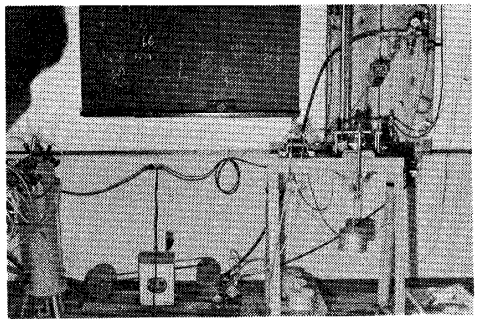

Fig. 8. Dynamic simple shear test apparatus

By this apparatus, dynamic shearing force can be applied; its main part is shown in Fig. 8 and the schematic diagram is given in Fig. 9(a).

The shearing box is installed in the pedestal 7.5 cm in diameter ② fixed on to the horizontal carriage ①. That is, a rubber sleeve of diameter 7.5 cm is set on the pedestal, fastened with an O-ring. And a ring holder of Delrin ③ is placed around the periphery, so that the O-ring on the pedestal is tightened against from the outside; water-proof between periphery of the pedestal and rubber sleeve is thus achieved. On the ring holder are then stacked 12 to 14 acryl ring ④, each of 75.2 mm in inner and 96.0 mm in outer diameter, and 2.0 mm thick, with the rubber sleeve positioned within the stack of rings.

The sample, of 75 mm in diameter and about 20 mm high, is then to be formed in the rubber sleeve. After establishment of the formed sample, the top cap (75 mm in diameter) ⑤ is placed on it, to which the upper edge of the rubber sleeve is fastened through an O-ring. Water-proofing there is achieved by tightening with a hose clamp above it.

A rod with its top socket for a vertical load is connected to the top cap; on this semi-spherical seat is placed a suspension-type weight. The (loading)

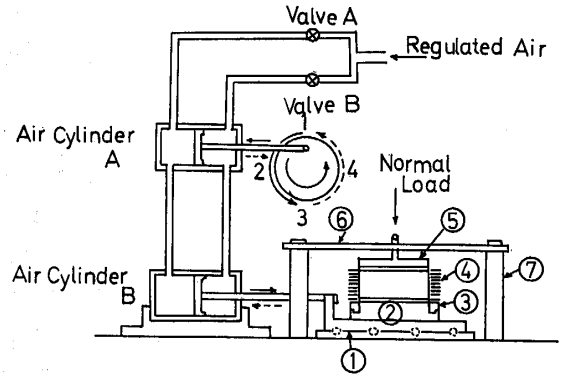

Fig. 9(a). Mechanism of dynamic simple shear test apparatus

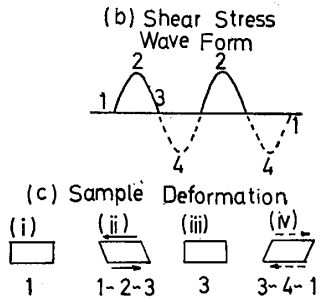

Fig. 9(b). Shear wave form
Fig. 9(c). Sample deformation

rod penetrates through the fixing plate ⑥ above at the middle; there is no clearance in this hole to permit horizontal movement of the upright rod. The fixing plate is supported in position by means of the four columns.

Since the top cap is fastened as just described, shearing force can thus be applied to the sample by moving the carriage horizontally left and right repeatedly.

In order to prevent slipping between sample and top cap and the pedestal during an experiment, a porous metal sheet with crisscross shallow grooves, 2 mm in thickness, is attached on the surface of both top cap and pedestal.

Between the horizontal carriage and the support plate below it are inserted ball bearings to nullify the friction between.

For applying the repeated shearing force to the sample, a double-action cylinder similar to that used in the dynamic triaxial test is utilized. A plate spring, 4 mm in thickness by 20 mm wide by 105 mm long, is inserted between the piston rod and the coupling to the carrige. And a wire strain gauge is attached to this spring; the shearing force applied to the sample is thus observed by mean of the strain occurring in this plate spring. In the apparatus, to give the load of shearing force in sinusoidal wave, the mechanism shown in Fig. 9(a) is employed. Two air cylinders A and B are connected in parallel. At first, the piston is positioned at the middle in each of the cylinders. And then, the valves A and B are opened at the same time, and compressed air of a specific pressure coming through a reducing valve is fed into the two cylinders.

Then, the valves A and B are closed simultaneously. In the air cylinder A, the piston rod is connected to an eccentric rod of eccentric radius 15 mm. As the result, the pressures in two chambers of this air cylinder are changed alternately and in sinusoidal manner by means of the revolution of the eccentric rod. In consequence, push and pull of the piston rod in the air cylinder B are similarly in sinusoidal waves, and hence the repeated shearing forces to the sample also sinusoidally.

These waves of shearing force are represented in Fig. 9(b), and the deformations of sample in (c). In the latter figure, the numbering 1, 2, 3, 4 corres-

pond to the positions of the eccentric rod numbered appropriately. The oscillation frequency can be changed by means of the number of revolutions of the eccentric rod; in this experiment, however, it is of 0.5 c/s, the same as in the case of dynamic triaxial test.

For measurement of the pore pressure, the pore water through the porous metal sheet on top of the pedestal is led to a pore pressure gauge through a polyethylene pipe. The pressure gauge used is of the same type as used in dynamic triaxial test.

Shearing displacement of the sample is obtained by measuring the displacement of the horizontal carriage. This displacement meter used is also that type used in triaxial test.

Experimental procedures

Dynamic triaxial test Compared to the case of shaking sand box, the sample in dynamic triaxial test is small in size, so that the sample must be perfectly saturated (this is also the case for simple shear test). For this reason, sand is placed in a conical flasket filled with water, which is then boiled for about one hour to remove completely air from the sand.

In forming the final sample, to prevent entry of air into it, the procedure indicated in Fig. 10 is used. The reason for this also for obtaining a loose sample, as well as the purpose already mentioned.

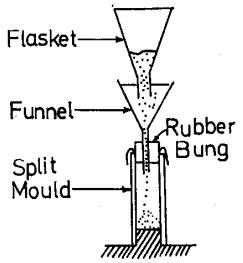

Fig. 10. Sample preparation

The rubber sleeve is fastened firmly on end to the pedestal, and a split mould is then set around it. The upper end of the rubber sleeve is pulled upward and then bent so as to be hooked on the upper end of the mould. As shown in Fig. 10, the rubber plug with a funnel is inserted into the top of the mould. Both the funnel and the mould are then filled with deaired water; and a stopper is set at the bottom of the funnel. The sand already prepared is introduced into the funnel, which is then stirred sufficiently to remove perfectly the contained air bubbles. The stopper is now removed, and sand grains settle down gently through water, accumulating in the mould. After complete packing of the mould, the rubber plug is removed, and the top cap is placed on top of the sample, which is then fastened tightly to the rubber sleeve. Pressure in the sample is adjusted to a negative pressure of about 4 cmHg, so that the sample

will stand by itself. The mould is removed, and the dimensions of the sample are taken. The triaxial cell is assembled, and the sample is consolidated suitably by means of the confining pressure. A connection is then made from the top cap to the piston rod of the air cylinder.

By manipulation of the reducing valve, the pressure of compressed air to the air cylinder is adjusted. Adjustment are made of the deviator stress meter, displacement meter, pore pressure meter, etc. Finally, by actuating the solenoid valve, deviator stress is applied repeatedly to the sample until liquefaction takes place in the sample sand.

The various quantities under study are recorded in pen-written oscillograph.

Dynamic simple shear test The horizontal carriage is set in position (with the piston in the air cylinder B taking its neutral position). A rubber sleeve for 7.5 cm diameter used is placed on the pedestal suitably, being tightened to the latter with an O-ring. The ring holder is then set, and 12 to 14 acryl rings are stacked on it, with the rubber sleeve within the stack. Top end of the rubber sleeve is bent outward so as to be hooked by an acryl ring.

Deaired water in suitable quantity is introduced into the rubber sleeve, and then the saturated sand deaired similarly to the case of triaxial test is pured gently through it.

Surface of the sand sample prepared is smoothed evenly, and the top cap is placed on it; the cap is connected tightly to the rubber sleeve with an O-ring. The top cap is fixed by means of the fixing plate above it. The drain cock is closed and the pore pressure meter is put into operative state, and consolidating pressure is then applied. It is confirmed that the pore pressure appearing is almost equal to the applied consolidating pressure. Subsequently, the drain cock is opened and the consolidation is again made. By measuring the amount of drain water, the initial void ratio is obtained. After completion of this compaction (i.e. the consolidation), the drain cock is again closed. The valves A and B in Fig. 9(a) are opened simultaneously, to supply specific air pressure to the two air cylinders, which is followed by closure of the valves. Shearing stress is thus repeatedly applied to the sample sand by operating an electric motor, until liquefaction occurs in the sample.

The various quantities such as shearing force, shearing displacement and pore pressure are recorded in pen-written oscillograph.

Experimental results and the discussion

Results of the dynamic triaxial test Fig. 11 shows the experimental results for the Shingu sand consolidated at void ratio $e=0.81$ (relative density $Dr=26\%$) with the initial, effective confining pressure $\sigma_3=1.0\,kg/cm^2$ and repeated deviator stress $\sigma_d=0.33\ kg/cm^2$.

As seen in the figure, there is no appreciable change in the axial strain up to the compression in the 21st cycle of repeated deviator stress. But in the

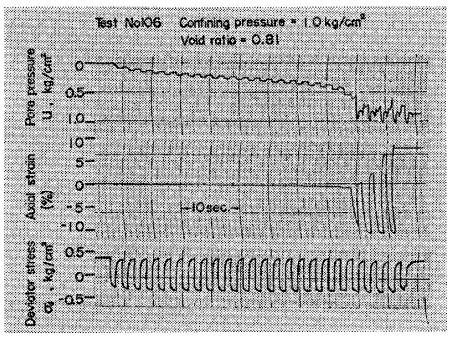

Fig. 11. Record of dynamic triaxial test

tension, the axial strain rises abruptly to 9%. In the subsequent 22nd cycle, axial strain also occurs in compression. And in the ensuing two to three cycles, the axial strain increases greatly, indicating the sample is no longer resistant to the deformation. That the values indicated at the 22nd cycle and thereafter are the same in tension is because the displacement in sample exceeds the range of the displacement meter, so that the meter cannot follow changes in the quantity. In actuality, the axial strains are over those indicated.

The pore pressure increases at a constant rate up to the compression in the 21st cycle; but no appreciable axial strain is observed in the sample. When a certain value of the pore pressure is reached, however, the axial strain starts to increase considerably. In the subsequent cycle, the pore pressure thus increases abruptly, the value being almost equal to the confining pressure.

As seen above, in a loose sand such as was used in the present experiment, the liquefaction is induced by an abrupt increase of the axial strain. And in the ensuing to three cycles, it is completely liquefied due to the deviator stress applied. This situation is illustrated by Mohr circles in effective stress, in Fig. 12. The circle at the 1st cycle of deviator stress is represented by (a). Due

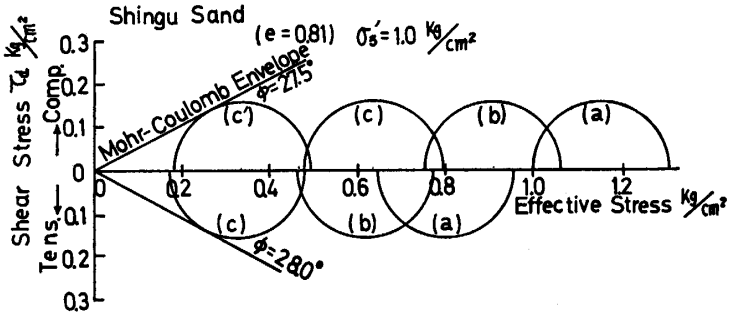

Fig. 12. Effective stress conditions on loose Shingu coarse sand

to the pore pressure then occuring, the circle is shifted by the amount U= 0.05 kg/cm². Then, in the 10th cycle, the Mohr circle (b) shift to the at (b) by the amounts U=0.25 kg/cm² (in compression) and U=0.23 kg/cm² (in tension) corresponing to the 10th cycle of deviator stress. At this point, however, no large deformation is observed in the sample, showing that liquefaction has

not yet taken place. In the 21st cycle, the circle has now shifted to (c). The pore pressure occurring up to this point is U=0.52 kg/cm² (both in compression and tension). What is greatly noteworthy here is that this pore pressure does cause an appreciable axial strain in the compression, but induces a large strain in the tension. That is to say, the sand sample has entered an initial liquefaction by this pressure on the side of tension.

In the ensuing 22nd cycle, the pore pressure increases abruptly in compression, with U=0.82 kg/cm², and an appreciable change in the axial strain is observed. The sand sample is thus liquefied on both compression and tension in this cycle. The Mohr circle in the liquefaction is given at (c′). This point where the initial liquefaction has occurred may be taken as a failure. And the angles of internal friction in the sample, as obtained from the Mohr-Coulomb envelope, are 28° in tension and 27.5° in compression; these values are nearly the same. This thus can be considered as a dynamic angle of the internal friction.

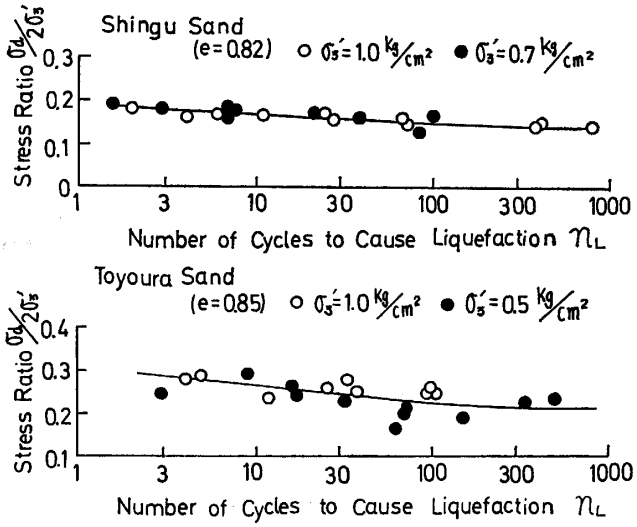

Fig. 13. Stress ratio $\sigma_d/2\sigma_3'$ required to cause liquefaction

In summarizing the results thus obtained, Fig. 13 shows the relation between the ratio $\sigma_d/2\sigma_3$, the maximum shearing stress (1/2 of the deviator stress σ_d) and the initial effective pressure respectively, and the munber of cycles, n_L, initiating liquefaction in the sample. For the Shingu sand, the void ratio is e=0.82 and for the Toyoura sand it is e=0.85. The initial effective pressures σ_3' are 0.7 and 1.0 kg/cm² for the Shingu and 0.5 and 1.0 kg/cm² for the Toyoura sand; no significant diffreences, however, are observed. In the experiment performed, it was again confirmed that, for a given void ratio, occurrence of the liquefaction is determined by the ratio of shearing stress and initial effective pressure.

Results of the dynamic simple shear test Figure 14 shows the results of simple shear test on the Shingu sand, with normal pressure 0.5 kg/cm² and void ratio

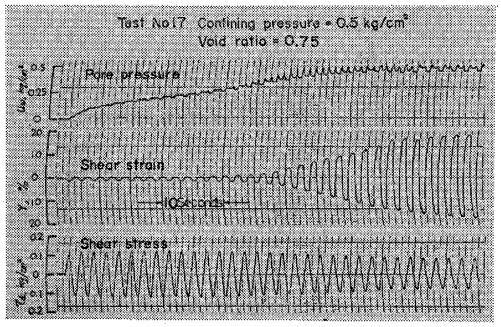

Fig. 14. Record of dynamic simple shear test

0.75 (relative density 48%).

In the previous experiment with a shaking sand box, the void ratio used was 0.82. Therefore, an attempt was made to have the same value, but owing to a shallow depth of the sand box, a loose Shingu sand with void ratio exceeding 0.75 could not be obtained. For the Toyoura sand, however, the void ratio was 0.85.

As seen in Fig. 14, the course taken up to occurrence of the liquefaction in simple shear test is similar to that in triaxial test. That is with increase in the number of cycles, the pore pressure in sample rises, and the effective stress in sample decreases correspondingly. And up to a certain number of cycles, the shearing displacement in sample is small, but subsequently the shearing strain increases abruptly, thereby leading to the liquefaction.

According to the results observed, it appears that, in the number of cycles from 16 to 17, the initial liquefaction has been caused. At the same time, the amplitude of repeated shearing force has started to decrease, indicating the loss of shearing resistance by the sample. The pore pressure then increases with hardly any amplitude up to occurrence of a large shearing strain, but as the strain has grown large, the wave form of the pore pressure is something like 1/2 the period in the repeated shearing stress.

This is because when the sample is displaced due to repeated shearing stress, the dilatancy become positive relatively, regardless of the sign (positive or negative) in shearing displacement. This can be understood from the fact that the through in wave of the pore pressure corresponds to the positive and negative maximum in shearing displacement of the sample.

Similarly to the case of triaxial test, the pore pressure at the time of an initial liquefaction was obtained and the degree of internal frinction at the failure due to effective stress was derived. The value for the Shingu sand is 24° and for the Toyoura sand it is 25°, both being somewhat smaller than those in triaxial test.

Figure 15 shows the relation between the ratio of shearing stress and initial effective pressure, i.e. τ_d/σ'_v, and the number of cycles causing liquefaction, n_L; this is based on results such as in Fig. 14.

The initial, effective normal pressure is only 0.5 kg/cm² for the Shingu sand, and it is both 1.0 and 0.5 kg/cm² for the Toyoura sand. The void ratio

is then 0.85 for the Toyoura and 0.75 for the Shingu sand.

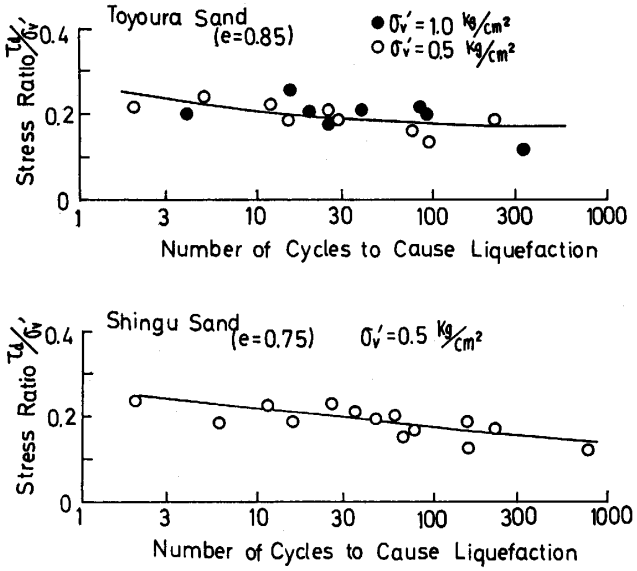

Fig. 15. Stress ratio τ_d/σ'_v required to cause liquefaction

Comparison between the respective experimental methods

The results of dynamic triaxial test and dynamic simple shear test, performed in order to assess the results of the shaking sand box test previously made, have been described. As also pointed out by Seed et al.[1], it was confirmed in both of these experiments that the smaller becomes the number of cycles causing the liquefaction, the less the initial effective pressure and the larger the repeated shearing stress. Some results were also obtained on the effect of sand density upon the liquefaction, which, however, will be omitted in the present report since the matter is not directly concerned with the present purpose.

It appears reasonable that the comparison between sand box test, dynamic triaxial test and dynamic simple shear test should be made in terms of the relation between the ratio of repeated shearing stress τ_d and initial effective pressure σ'_v, on one hand, and the number of cycles causing liquefaction n_L, on

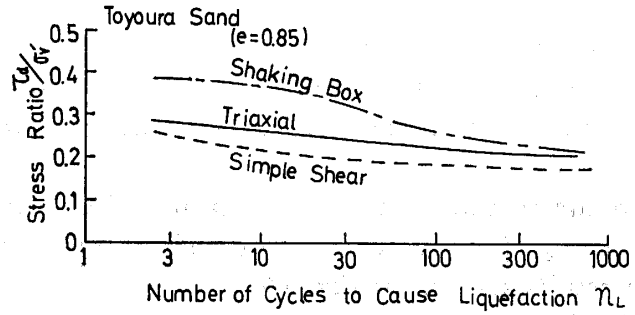

Fig. 16. Comparison of stress ratio τ_d/σ'_v required to cause liquefaction in three different tests

the other, for a given void ratio in sand sample.

Figure 16 shows the results of the three respective tests on the Toyoura sand with a void ratio of 0.85 (the relative density 58%).

Figure 17 shows similar results for the Shingu sand. For this sand, however, the comparison could not be made for the same void ratio, Therefore, for between shaking sand box and dynamic triaxial tests, the void ratio is 0.82 (relative density 23%), and for between dynamic triaxial and dynamic simple shear tests it is 0.75 (48%).

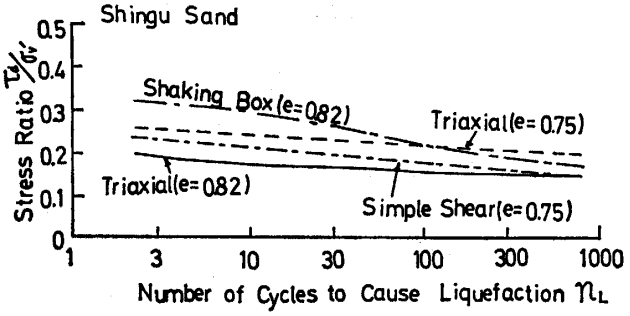

Fig. 17. Comparison of stress ratio τ_d/σ_v' required to cause liquefaction in three different test

The results by sand box test were obtained with the frequency in 4 c/s which deffers from 0.5 c/s for both the triaxial and simple shear tests. In regard of this point, Peacock and Seed made experiments with frequencies from 1/6 to 4 c/s, and reported the effect of a change in the frequency on the liquefaction is insignificant in this range.[1] In the figure 16 and 17, therefore, for the results by sand box test the values in horizontal axis of Fig. 5 are converted to the numbers of cycles.

Furthermore, the angle of internal friction in sand sample, used in deriving Fig. 5 from Fig. 3 for the results by sand box test, is 34° for the Toyoura and 30° for the Shingu sand, as already described. To obtain these values, the experiment made, mentioned earlier in the present report as "will be described the experiment made, mentioned earlier in the present report as "will be described later", is as follows.

The experiment is called by the author as the ECU test in triaxial compression test; it is a test with the stress controlled. In this procedure of experiment, the sand sample is first consolidated isotropically by a specific confining pressure σ_3. And then, by means of a suspension weight, the additional deviator stress σ_d is applied. Back pressure is applied through the sample pedestal, thereby raising the pore pressure in sample gradually.

The effective stress in the sand sample thus decreases gradually, and eventually a shear failure of the sample occurs at a certain shearing stress.

This situation is represented by Mohr circles in Fig. 18. Circle (a) is the stress condition when the deviator stress σ_d is applied after consolidation with

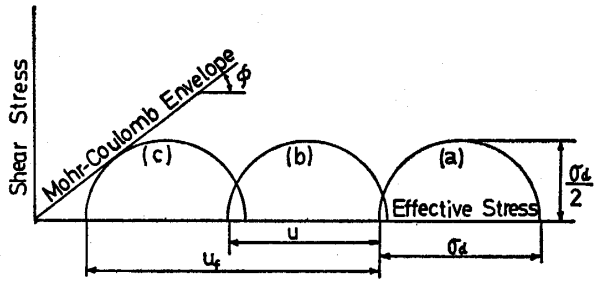

Fig. 18. Effective stress condition of ECU–Test

confining pressure σ_3. As the pore pressure in samples is increased gradually, the condition (b) is attained. When it becomes U_f, the circle (c) is reached. At this time, the Mohr circle comes in contact with the Mohr-Coulomb envelope. This situation of failure can be observed through the axial strain as the pore pressure is increased; that is, when a certain value of the pore pressure is reached, the axial strain suddenly increases. The course taken is more gradual as the density of sample sand is larger.

These results are shown in Fig. 19 as an example. The failure evidently occurs at a point where the axial strain increases suddenly. In the case of a

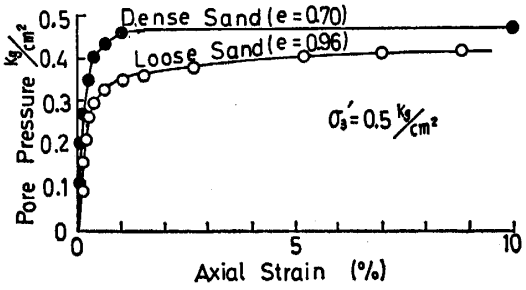

Fig. 19. ECU–Test result on Toyoura fine sand

loose sand, however, the change in axial strain is gradual. In Fig. 19, the point when the curvature in curve is the largest is thus taken as that of the failure.

Therefore, the angle of internal friction is obtained as follows. From the pore pressure at the point of failure, the Mohr circle such as (c) in Fig. 18 is first obtained. Then, assuming there is no cohesion in the sample (hardly any cohesion is observed by experiment), the angle of internal friction is derived from the slope of a straight line tangential to this Mohr circle.

These results obtained are shown in Fig. 20 by "ECU-Test"; the values by ordinary CU-test are also given as "SCU-Test".

The experiment described was made because, in liquefaction of the sand, shear failure occurs during the course of the pore pressure being increased gradually. The angles of internal friction were obtained under the condition approaching to this situation.

As seen in the figure, the values by ECU-test are smaller than those by CU-test; these smaller values were taken, as already described.

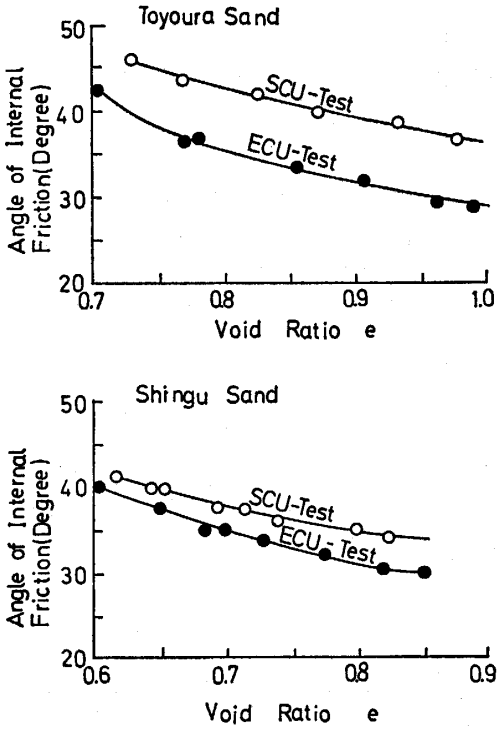

Fig. 20. Relationship between angle of internal friction and void ratio on consolidated undrained tests

Taking the situation such as above descrived into consideration, the results by the three respective techniques were compared, as already described. As seen from Fig. 16 and Fig. 17, for the same number of cycles causing liquefaction, the shearing stress required is largest with shaking sand box test, followed by triaxial test and simple shear test in order. (In Fig. 17, the void ratios are different, so that uniform comparison is not possible. The tendency observed, however, is similar to that in Fig. 16)

The reason for this is not clarified yet. The deviation between triaxial test and simple shear test, however, as also pointed out by Seed and by Finn[3], may be due to the differences in the direction of principal stress, maximum principal stress and average principal stress. Then, for sand box test, causes may be in similar affairs, and also in limitation of the box itself, as well as in the particular angle of internal friction used.

This situation causing the differences may be seen by the comparison in the angle of internal friction between the respective experiments, shown in Fig. 21. The angles of internal friction by ECU-test are larger than those in occurrence of the liquefaction by both dynamic triaxial and simple shear test. If now the results by sand box experiment (for the Toyoura sand) are treated with the angle of internal friction, 25°, obtained by simple shear experiment, the values become very close to those by the other two tests, viz. dynamic triaxial test and dynamic simple shear test, as seen in Fig. 22.

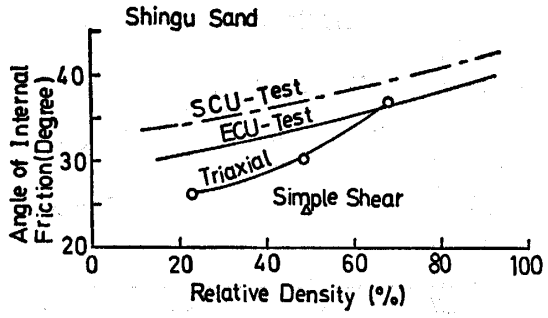

Fig. 21. Comparison of angle of internal friction determined by dynamic and static tests

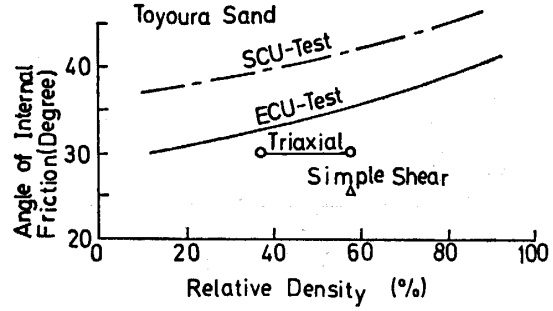

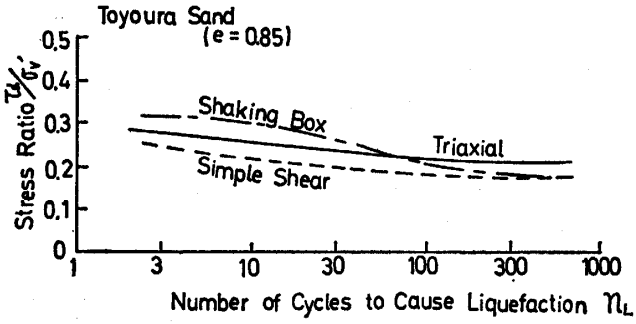

Fig. 22. Comparison of stress ratio τ_d/σ'_v required to cause liquefaction in three different tests

Conclusion

In order to evaluate the results on liquefaction of the saturated sand by shaking sand box test, dynamic triaxial test and dynamic simple shear test have been made for the same sands. By comparison between the three respective tests, the following are concluded.

(1) In each of the three experiments, occurrence of the liquefaction is determined simply by the ratio τ_d/σ'_v, the repeated shearing stress and the initial, effective confining pressure, respectively.

(2) For the same number of cycles causing liquefaction, the value of τ_d/σ'_v required is largest with sand box test, followed by triaxial test and simple shear test in order. With the value by sand box test as 100%, the value by triaxial

test is about 80% and by simple shear test 68%. The primary cause for the discrepancies may be in the angles of internal friction used.

Acknowledgement

The author is deeply indebted to Mr. Naohiko Suzuoka, a graduate student in the author's university, for his aid in the present experiments and his helpful discussion.

Symbols used in the paper

e : Void ratio
n_L : The number of cycles causing liquefaction
t_L : Shaking duration causing liquefaction
U : Pore pressure
U_f : Pore pressure in initial liquefaction
ϕ : The angle of internal friction
τ_d : Repeated shearing stress
ϕ_d : Repeated deviator stress
σ_3 : Confining pressure in triaxial test
σ_3' : Initial effective confining pressure
σ_v' : Initial effective normal pressure

References

1) H. B. Seed and K. L. Lee: Proc. ASCE, **92,** SM6, 105~134 (1966).
W. H. Peacock and H. B. Seed: Proc. ASCE, **94,** SM3, 689~708 (1968).
2) S. O-hara and N. Suzuoka: Soil Mechnics and Foundation Engineering, **20, 5,** 45~50 (1972) (in Japanese).
3) W. D. L. Finn, D. J. Pickering and P. L. Bransby: Proc. ASCE, **92, SM4,** 639~659 (1971).